Cluster Models for Calcite Surfaces: Ab Initio Quantum Chemical Studies

Henna Ruuska, Pipsa Hirva,* and Tapani A. Pakkanen

University of Joensuu, Department of Chemistry, P.O. BOX 111, FIN-80101, Joensuu, Finland

Received: March 5, 1999; In Final Form: June 8, 1999

Cluster models for the calcite ($CaCO_3$) (001) surface were calculated by the ab initio Hartree−Fock method with the purpose of developing a model for studies of local surface reactions such as adsorption. The models were evaluated in terms of their density of states and charge distribution. The termination of a naked cluster model is important, and two methods of stabilizing the models were considered. An array of point charges, a method of stabilizing ionic models, was tested and found to work poorly. An alternative method was then tested in which cluster models of semi-ionic surfaces were stabilized by surrounding the cluster with water molecules. The water molecules around the cluster increased the stability of the model substantially and also made the model more realistic. An estimate for the energy of adsorption of water to the (001) surface of calcite is presented.

1. Introduction

Calcium minerals are important raw materials in the chemical and construction industries and in agriculture. A widely used separation method for calcium minerals is flotation, which is based on the interaction between the mineral surface and the collecting molecule.[1,2] To increase the effectiveness and selectivity of flotation, we need to understand the adsorption mechanisms of the collector. This process can be studied by applying computational methods at the atomic level.

One quantum chemical approach to modeling solid surfaces is to treat the surface as an infinite periodical slab. Another is to describe the surface as a cluster of atoms. This second approach, which is the one applied here, allows the local character of the chemical bond between surface and adsorbate to be taken into account. Problems associated with the cluster method are the need to terminate the cluster and the incomplete description of the effects of the surrounding bulk lattice.[3] Cluster models are widely used in studying metal surfaces,[4] covalent compounds,[5,6] and strongly ionic surfaces such as MgO and NaCl.[7−9] Different methods of terminating the cluster are used, depending on the nature of the system. Cluster models of covalent compounds are often terminated with hydrogens in order to eliminate the border artifacts. In the case of fully ionic surfaces, in turn, the electrostatic potential of the extended crystal is often taken into account by embedding the cluster in an array of point charges. However, one problem with this method is the polarization of anions near the borders of the cluster.[10−11]

Semi-ionic surfaces such as these of calcium minerals have not been investigated extensively by computational methods. Beck et al.[12] have investigated the electronic structure and Parker et al.[13] the binding energies and charge density of calcium carbonate with periodical ab initio calculations. Lattice properties and the electronic structure of fluoroapatite have been calculated by applying a local-density-functional pseudopotential approach.[14] The cluster approach with a very small cluster model (PO_4^{3-} or CO_3F^{3-}) in a point-charge array has been used in ab initio calculations in studies of the ion substitution mechanism in carbonate fluorapatite.[15] Simulation techniques have been applied in studies of calcite morphology[16] and interaction of the minerals calcite and fluorite with water and methanoic acid.[17] Although ab initio methods with the cluster approach are useful in investigating local phenomena such as adsorption to a mineral surface, the computational requirements are high and the studies must be limited to small models. A small naked cluster model is very reactive, however, and termination of the cluster is important. Methods of stabilizing small cluster models are considered in this work.

The aim of our work was to investigate cluster models suitable for modeling the adsorption interaction for calcite. Five cluster models of formula $Ca_n(CO_3)_n$ were calculated with ab initio HF/3-21G level of theory, and the performance of these models and the cluster termination methods are discussed. The applicability of the point-charge array for the semi-ionic calcite was tested, as well as an alternative method where the cluster was surrounded with water molecules.

2. Theoretical Methods

Calculations were carried out by using the ab initio Hartree−Fock (HF) method with the basis set 3-21 G. Quantum mechanical calculations of the cluster models of semi-ionic surfaces were time-consuming because of the slow SCF convergence. The slow convergence is due to the instability of an isolated cluster. In general, the convergence was even slower with density functional methods, so at this stage only the Hartree−Fock method was used. The HF/3-21G level of theory makes calculations of bigger cluster models feasible and was used for testing the models. In addition to the common Mulliken population analysis, the charge distributions were computed with the CHELPG method,[18] which calculates the molecular electrostatic potential and fits it to a series of point charges placed at the atomic centers. Cluster models, described in more detail in the next chapter, were constructed with the molecular

* Author to whom correspondence should be addressed. E-mail: Pipsa.Hirva@joensuu.fi.

10.1021/jp990793f CCC: $18.00
Published on Web 07/27/1999

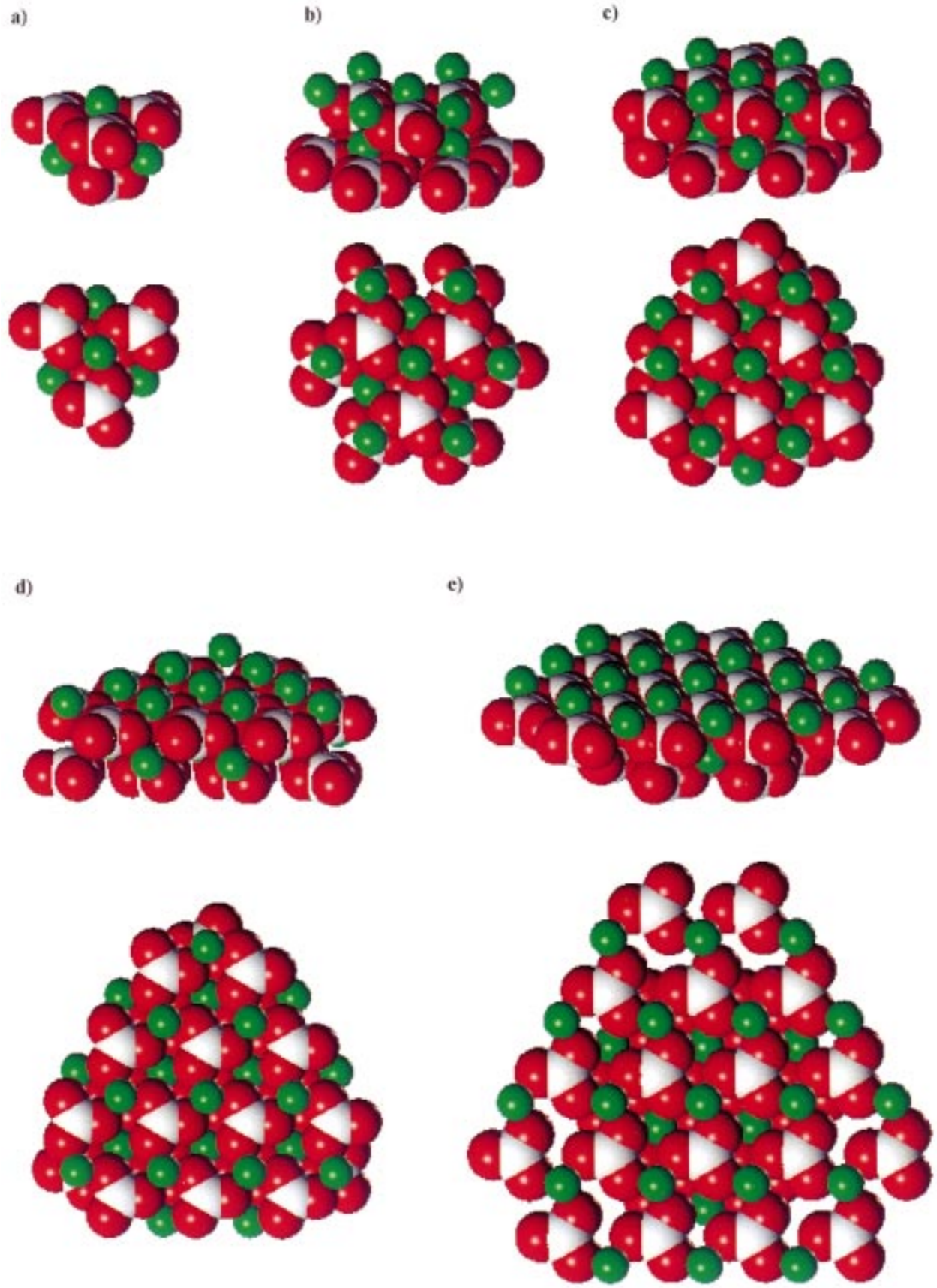

Figure 1. Cluster models of the $Ca(CO)_3$ (001) surface viewed from the side and the top: (a) $Ca_4(CO_3)_4$, (b) $Ca_{10}(CO_3)_{10}$, (c) $Ca_{13}(CO_3)_{13}$, (d) $Ca_{22}(CO_3)_{22}$, and (e) $Ca_{25}(CO_3)_{25}$. Ca = green; C = white; O = red.

modeling program SYBYL[19] by cutting them from the bulk structure of calcite.[20] All ab initio calculations were performed using the program *Gaussian94*[21] on a Silicon Graphics Origin200 R10000 4-processor workstation.

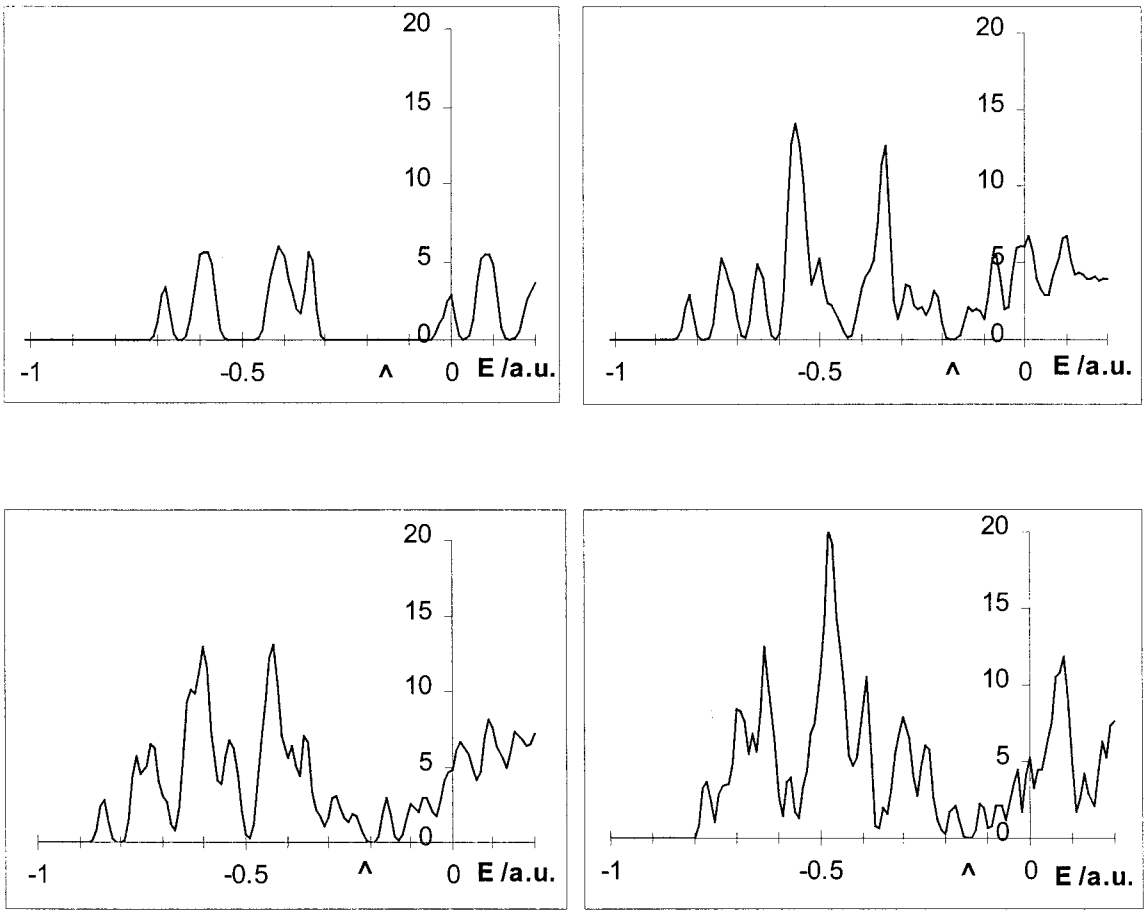

Figure 2. DOS curves of cluster models $Ca_4(CO_3)_4$, $Ca_{10}(CO_3)_{10}$, (top panels) and $Ca_{13}(CO_3)_{13}$, and $Ca_{22}(CO_3)_{22}$ (bottom panels). The band gap between HOMO and LUMO orbitals is indicated with the symbol ∧.

3. Results

Models. The ultimate goal of this work was to find a good model for an adsorption site on calcite. The crystal structure of calcite is rhombohedral. The plane considered was the (001)-plane, which is densely packed and consists of calcium atoms each coordinated to three carbonate groups below. The cluster models were stoichiometric including the same number of calcium atoms and carbonates. All models consisted of two calcium and two carbonate levels and they were made as symmetrical and smooth as possible.

Five models of different sizes were cut from the bulk structure of calcite: $Ca_4(CO_3)_4$, $Ca_{10}(CO_3)_{10}$, $Ca_{13}(CO_3)_{13}$, $Ca_{22}(CO_3)_{22}$, and $Ca_{25}(CO_3)_{25}$, as shown in Figure 1. The smallest model consists of a single surface calcium atom and three underlying CO_3 groups in the two top layers. In the third layer there are three calcium atoms and at the bottom one carbonate. The model is compact but somewhat irregular on the sides. In the second model, $Ca_{10}(CO_3)_{10}$, the central calcium is not as naked as in the smallest model, but the ring of six calcium atoms is somewhat exposed. The next model, $Ca_{13}(CO_3)_{13}$, is more regular and not significantly bigger than the previous one.

The larger models were calculated to allow estimation of the charge distribution. The charges were subsequently used for the creation of an array of point charges to model the potential of the cluster surroundings. The $Ca_{22}(CO_3)_{22}$ model is regular and as symmetrical as possible. In the biggest model ($Ca_{25}(CO_3)_{25}$), the surface layer was made larger than the bottom layer, since the influence of the surface layer on the charge of the central surface calcium was expected to be greater than that of the bottom layer.

TABLE 1: Cohesion Energies $E(Ca_n(CO_3)_n)/n$ (the total energy per one $CaCO_3$ unit), Relative Cohesion Energies Related to the Most Stable Model $Ca_4(CO_3)_4$, and Charges of Central Surface Calcium of the Cluster Models of Calcium

$Ca_n(CO_3)_n$	$E(Ca_n(CO_3)_n)/n$ (au)	$\frac{E_n}{n} - \frac{E_4}{4}$ (kJ/mol)	Mulliken charge of surface Ca	CHELPG charge of surface Ca
$Ca_4(CO_3)_4$	−934.583884	0	1.521	1.933
$Ca_{10}(CO_3)_{10}$	−934.404844	470.1	0.839	1.202
$Ca_{13}(CO_3)_{13}$	−934.494635	234.3	0.818	
$Ca_{22}(CO_3)_{22}$	−934.566111	46.7	1.440	0.906
$Ca_{25}(CO_3)_{25}$	−934.510977	191.4	1.066	0.960

Except for $Ca_4(CO_3)_4$, the SCF convergence of these cluster models in ab initio calculations was slow, because of the instability of the isolated cluster. Problems were encountered especially with the $Ca_{13}(CO_3)_{13}$ model.

Evaluation of the Models. The cohesion energy of a model, the energy per one $CaCO_3$ unit, gives an indication of the stability of the model. On this basis, the smallest model $Ca_4(CO_3)_4$ is the most stable and $Ca_{10}(CO_3)_{10}$ the most unstable, as can be seen from Table 1. The table shows cohesion energies and the relative cohesion energies compared with the most stable model. Information about the stability of the cluster models can also be obtained by investigating their HOMO and LUMO energies and the density of energy state (DOS) diagrams. This information was important in trying to understand the slow convergence of the models.

Except for the $Ca_4(CO_3)_4$ model, the band gap between the HOMO and LUMO orbitals is small. This causes problems with the SCF convergence in calculations, since the method cannot

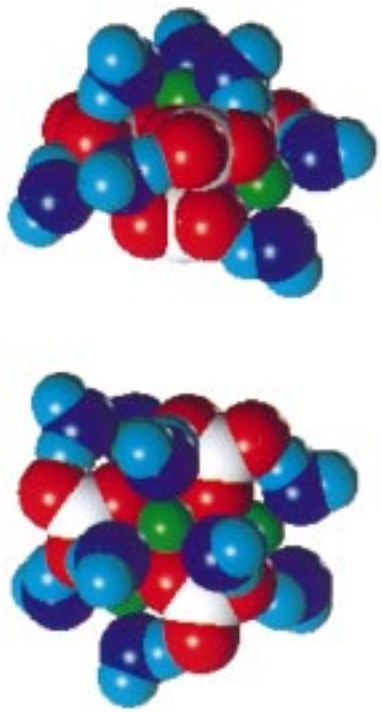

Figure 3. Side and top views of $Ca_4(CO_3)_4/9H_2O$. The positions of the nine water molecules are optimized. Ca = green; C = white; O in CO_3 = red; O in H_2O = dark blue; H = light blue.

easily find the ground state of the system. The band gap of a neutral molecule or model should be located in the vicinity of zero energy. However, as can be seen from Figure 2, the virtual orbitals of the models are negative, indicating the instability of the model. Especially in the $Ca_{13}(CO_3)_{13}$ model a second deep gap in the DOS curve can be seen near the Fermi level. This is related to the very slow convergence of the model, for it is difficult to choose the ground state from among the possible states.

Another way of evaluating cluster models is to observe the atomic charge distribution. We calculated the atomic charges by two different methods: Mulliken population analysis and the CHELPG method. The charges of the central calcium atoms of the five models are presented in Table 1. Contrary to desire, the charges did not change regularly as the size of the model was increased. This was probably due to the variable shapes of the models. The Mulliken charges of $Ca_4(CO_3)_4$ and $Ca_{22}(CO_3)_{22}$ are closely similar. In general, the Mulliken charges were more regularly distributed, and the most regular distribution was obtained with the $Ca_{22}(CO_3)_{22}$ model. The charges of the surface layer in the $Ca_{25}(CO_3)_{25}$ model were irregular, owing to the small bottom layer.

Stabilizing the Cluster Models. The electrostatic field of the surrounding crystal in the cluster models of ionic materials is often taken into account by embedding the cluster in an array of point charges. When the compound is strongly ionic, the total ionic charges can be used as the values of charges, but for semi-ionic surfaces such as calcite, fractional charges are needed. Choosing the values of the fractional charges is not straightforward. To get an idea of the charge distribution, we calculated the atomic charges of five cluster models differing in size by two different methods. As mentioned above, the atomic charges

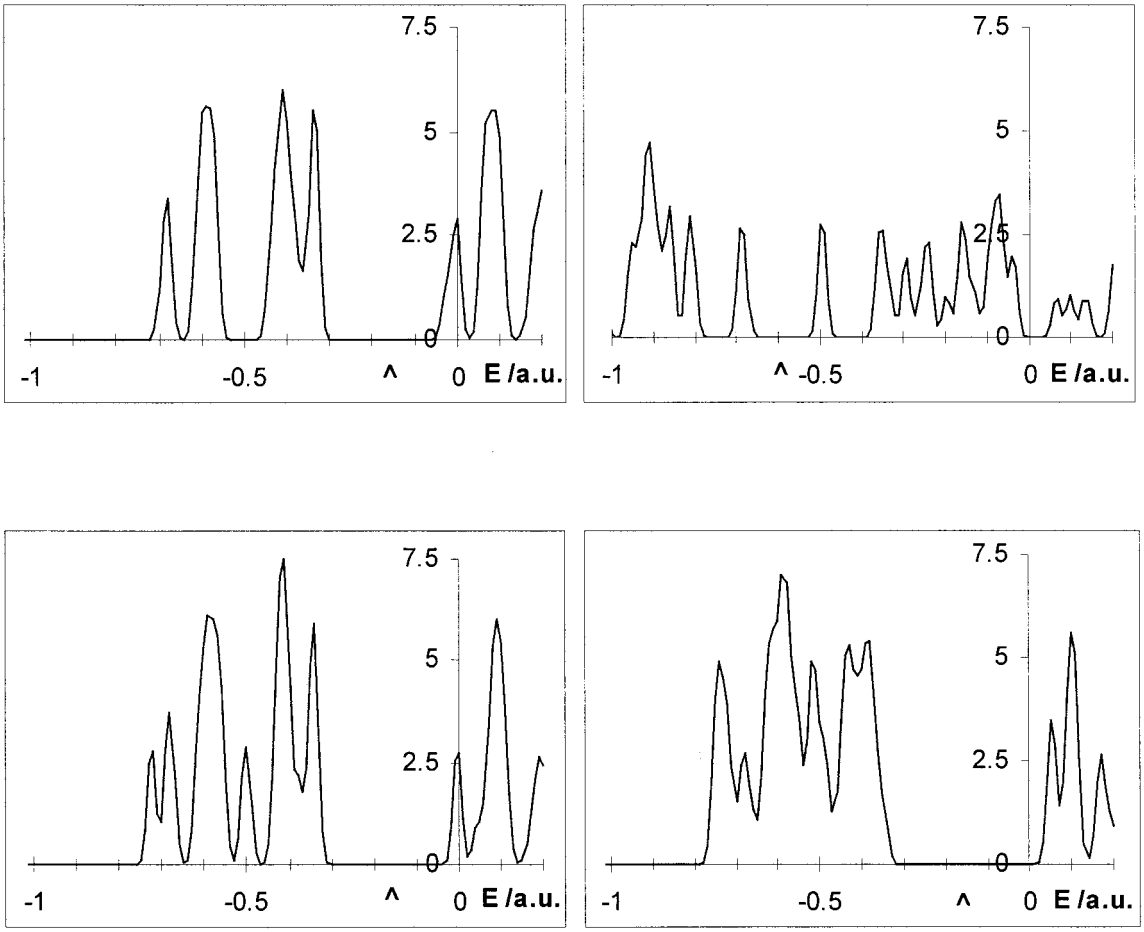

Figure 4. DOS curve of naked $Ca_4(CO_3)_4$ model and $Ca_4(CO_3)_4$ with an array of 45 × ±1.4 point charges (top panels) and $Ca_4(CO_3)_4$ with three and nine waters (bottom panels). The band gap between HOMO and LUMO orbitals is indicated with the symbol ∧.

of the calcite cluster models did not change regularly with the cluster size, so it was difficult to choose the values of charges. Three values (±1.0, ±1.2, ±1.4) were tested with an array of different dimensions.

The smallest model $Ca_4(CO_3)_4$ was used in testing the array of point charges. Positive and negative charges of the same absolute value were placed at sites where the next Ca and C atoms (centers of carbonate ion) would be located in the crystal structure. The values of the charges at C atoms were approximated as an average value of the whole CO_3 ion. First, 9, 18, and 21 negative and positive point charges in two layers were applied corresponding thus to the shape of the $Ca_{13}(CO_3)_{13}$ and $Ca_{22}(CO_3)_{22}$ models, and to one larger array of the same shape as the $Ca_{22}(CO_3)_{22}$ model. For a still larger array, 45 positive and negative point charges were taken, forming a regular array to the sides and below the $Ca_4(CO_3)_4$ model.

The point charge array affects the shape of the DOS diagram of the model and the Fermi level shifts to lower energy, further away from zero level, as can be seen in Figure 4. The band gap becomes narrower and the charge of the central surface calcium increases as the absolute value of the point charges and the size of the array are increased. Tests with larger lattice (point charges corresponding to 96 fragments) and charges on individual atoms instead of average value of carbonate group had negligible influence on the DOS curves.

An alternative way of stabilizing the cluster model was studied as well: the cluster was surrounded with water molecules. Since water is present in the flotation process, some effects of the solvent could be considered and the model made more realistic. The method was first tested with the smallest model $Ca_4(CO_3)_4$. Three water molecules were placed at the surface of the cluster so that the oxygen atoms of the water were pointed toward the calcium atoms. The positions and configurations of the water molecules were optimized, while the structure of the cluster was held fixed. At optimization, the hydrogen atoms of the water molecules formed bonds with the low-coordinated oxygen atoms of the carbonate groups, while the oxygen atoms of the water stayed close to the calcium atoms. The DOS curve of this water-covered model is presented in Figure 4. The band gap was broadened and slightly shifted to the positive direction.

Next the $Ca_4(CO_3)_4$ cluster was fully surrounded by water molecules. In addition to the three molecules on the surface, six additional molecules were placed at the bottom of the model. The final positions of these nine water molecules after optimization are shown in Figure 3. Once again the hydrogen atoms formed bonds with the oxygen atoms of carbonate groups, but now the water molecules were removed farther from their original positions, and the final positions were not totally symmetrical. In a third step, three additional molecules were placed at the open sites, but the optimal positions for these twelve molecules were not found.

As can be seen from the DOS curve in Figure 4, all the virtual orbitals of the nine-water model are positive. As the values in Table 2 show, the band gap is a bit broader for the twelve-water model than for the nine-water model. From the charges of the surface calcium, also included in Table 2, it is evident that the value of the charge of the central calcium decreases when the cluster is surrounded by water molecules, but the difference between the models with nine and twelve molecules is negligible.

Even though the SCF convergence becomes faster with the water molecules included, it takes time to find the optimized positions of the molecules in bigger models. To take into account the natural thermal motion of the water molecules would require molecular dynamics calculations, but this was not within the scope of our study. Accordingly the effect of the optimal sites and configurations was investigated. The three water molecules on the surface of $Ca_4(CO_3)_4/9H_2O$ were removed and the energy

TABLE 2: HOMO and LUMO Energies, Band Gap, and Charges of the Central Surface Calcium of the Water-Stabilized Models

model	*E*(HOMO)/au	*E*(LUMO)/au	Δ*E*/au	Ca charge
$Ca_4(CO_3)_4$	−0.33246	−0.02640	0.30606	1.521
$Ca_4(CO_3)_4/3H_2O$	−0.33719	−0.00619	0.33100	1.239
$Ca_4(CO_3)_4/9H_2O$	−0.34798	0.04432	0.39230	1.259
$Ca_4(CO_3)_4/12H_2O$	−0.38113	0.04430	0.42543	1.257
$Ca_{10}(CO_3)_{10}$	−0.21521	−0.13925	0.07596	0.839
$Ca_{10}(CO_3)_{10}/9H_2O$	−0.24612	−0.15236	0.09376	1.028
$Ca_{10}(CO_3)_{10}/10H_2O$	−0.24382	−0.15086	0.09296	1.093

TABLE 3: Energies for Interaction of One Water Molecule with $Ca_4(CO_3)_4$ and $Ca_{10}(CO_3)_{10}$ Models

	E (kJ/mol)
$Ca_4(CO)_4$	−229.5
$Ca_4(CO_3)_4/6H_2O$/optimized	−235.5
$Ca_4(CO_3)_4/6H_2O$/partially optimized	−226.4
$Ca_{10}(CO_3)_{10}$	−183.7
$Ca_{10}(CO_3)_{10}/9H_2O$/partially optimized	−184.7

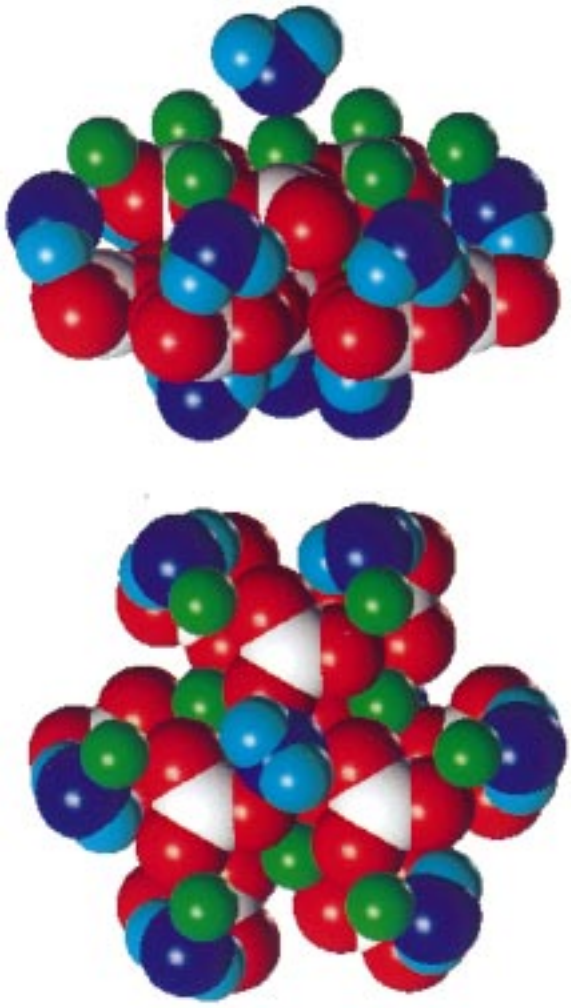

Figure 5. Side and top views of $Ca_{10}(CO_3)_{10}$ model surrounded by 10 water molecules. Ca = green; C = white; O in CO_3 = red; O in H_2O = dark blue; H = light blue.

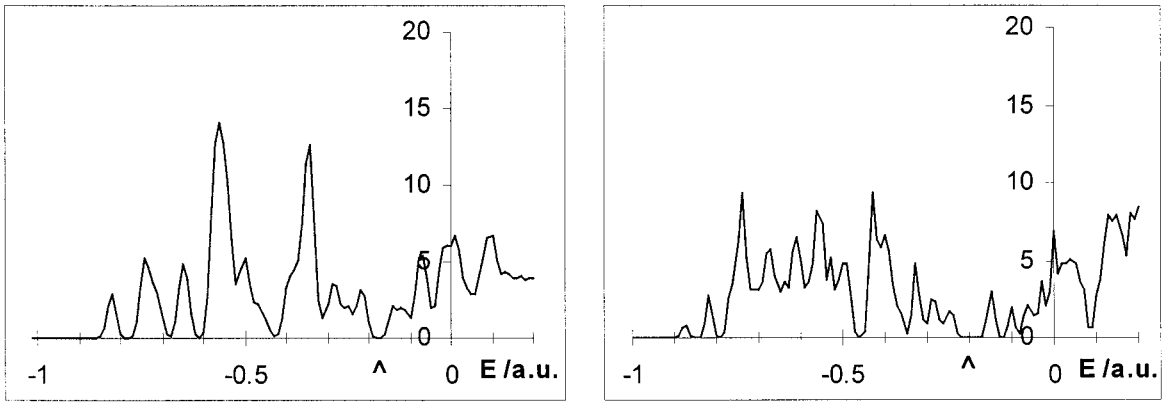

Figure 6. DOS curve of the naked $Ca_{10}(CO_3)_{10}$ model and $Ca_{10}(CO_3)_{10}$ with 10 water molecules. The band gap between HOMO and LUMO orbitals is indicated with the symbol ∧.

of adsorption of one water molecule to the surface was calculated. The positions of the six water molecules on the lower side of the model were either optimized or nonoptimized. In the nonoptimized situation, the molecules were originally placed in arbitrary but still reasonable positions. The interaction energies are presented in Table 3. The difference between the energies, 9 kJ/mol, is not significant in comparison with the large values of the energy, which means that there is no need to fully optimize the positions of the water molecules when the method is applied to bigger models. However, the water molecules should be located close enough to the model and hydrogen bonded to carbonate so that stabilization is achieved.

Surrounding a larger model with water molecules was investigated by placing 10 molecules around the $Ca_{10}(CO_3)_{10}$ model as shown in Figure 5. Six water molecules were first placed to the sides of the model and the positions were optimized. Three additional water molecules were placed to the bottom of the model, and partially optimized. Then a single water molecule was brought to the surface. The adsorption energy was smaller when the water molecule was adsorbed to the $Ca_{10}(CO_3)_{10}/9H_2O$ model than when it was adsorbed to $Ca_4(CO_3)_4/6H_2O$ (see Table 3). The DOS diagram of the $Ca_{10}(CO_3)_{10}/10H_2O$ is shown in Figure 6, and the band gap and surface calcium charge are presented in Table 2. The presence of the surrounding water molecules broadened the band gap and improved the SCF convergence time by a factor of 4.

4. Discussion

The most stable model, measured by the cohesion energies and DOS curves, was $Ca_4(CO_3)_4$. However, this model is small. The next model, $Ca_{10}(CO_3)_{10}$, was not very stable, and the more stable $Ca_{13}(CO_3)_{13}$ would be better if the SCF convergence could be improved. Although the $Ca_{22}(CO_3)_{22}$ model was also stable, it is too large to be practical in ab initio adsorption studies.

The commonly applied approach for ionic surfaces of using an array of point charges to stabilize the cluster models was not successful. Determination of the appropriate value of the charges and the extent of the array proved difficult. The point charge method had unfavorably strong influence on the electronic structure of the models and improved neither the stability nor the convergence properties of the cluster models. This failure results partially from the strong dipole moment caused by the point charge array and the fact that the point charges do not represent the spatial extent of the surrounding atoms.

Since the point charge method was found to work poorly for calcite models, an alternative method for stabilizing the semi-ionic clusters was developed. The placement of water molecules around the cluster speeded up the SCF convergence, enlarged the band gap between the HOMO and LUMO orbitals and shifted the band gap nearer to the zero energy, and so stabilized the model. A further advantage of this method is the opportunity to take into account some effects of the solvent, so that the model became more realistic. Because the water molecules increased the size of the model, the geometry optimization was slow with the bigger models. However, placement of the molecules in exactly optimal places was not necessary, as the solvent molecules stabilized the model and represented the influence of the solvent without full optimization. Surrounding the cluster with water molecules is a chemically reasonable approach to stabilize the model since it represents the situation where a small particle of calcite is in aqueous solution.

References and Notes

(1) Gallios, G. P.; Matis, K. A. In *Innovations in Flotation Technology*; Mavros, P., Matis, K. A., Eds.; Kluwer Academic Publishers: The Netherlands, **1992**; p 357.

(2) Holmgren, A.; Wu, L.; Forsling, W. *Spectrochim. Acta* **1994**, *50A*, 1857.

(3) Sauer, J. *Chem. Rev.* **1989**, *89*, 199.

(4) Yang, H.; Whitten J. L. *J. Phys. Chem. B* **1997**, *101*, 4090.

(5) Brown, R. C.; Cramer, C. J.; Roberts, J. T. *J. Phys. Chem. B* **1997**, *101*, 9574.

(6) Strandh, H.; Pettersson, L. G. M.; Sjöberg, L.; Wahlgren, U. *Geochim. Cosmochim. Acta* **1997**, *61*, 2577.

(7) Pacchioni, G.; Ferrari, A. M.; Márquez, A. M.; Illas, F. *J. Comput. Chem.* **1997**, *18*, 617.

(8) Pascual, J. L.; Pettersson, L. G. M. *Chem. Phys. Lett.* **1997**, *270*, 351.

(9) Yudanov, I. V.; Nasluzov, V. A.; Neyman, K., M.; Rösch, N. *Int. J. Quantum Chem.* **1997**, *65*, 975.

(10) Stefanovich, E. V.; Truong, T. N. *J. Chem. Phys.* **1997**, *106*, 7700.

(11) Masel, R. I. *Principles of Adsorption and Reaction on Solid Surfaces*; John Wiley & Sons: New York, 1996; Chapter 3.

(12) Beck, K. M.; McCarthy, M. I.; Hess, W. P. *J. Electron. Mater.* **1997**, *26*, 1335.

(13) Parker, S. C.; Oliver, P. M.; De Leeuw, N. H.; Titiloye, J. O.; Watson, G. W. *Phase Transitions* **1996**, *61*, 83.

(14) Louis-Achille, V.; De Windt, L.; Defranceschi, M. *Comput. Mater. Sci.* **1998**, *10*, 346.

(15) Regnier, P.; Lasaga, A. C.; Berner, R. A. *Am. Mineral.* **1994**, *79*, 809.

(16) Catti, M.; Pavese, A. In *Modelling of Minerals and Silicated Minerals*; Silvi, B., D'Arco, P., Eds.; Kluwer Academic Publishers: The Netherlands, 1997; p 113.

(17) de Leeuw, N. H.; Parker, S. C.; Hanumantha Rao, K. *Langmuir* **1998**, *14*, 5900.

(18) Breneman, C. M.; Wiberg, K. B. *J. Comput. Chem.* **1989**, *11*, 361.

(19) *Sybyl 6.2*; Tripos, Inc.: St. Louis, MO, 1995.
(20) Deer, W. A.; Howie, R. A.; Zussman, J. *An Introduction to the Rock-Forming Minerals*, 2nd ed.; Longman: Essex, 1992; p 623.
(21) Frisch, M. J.; Trucks, G. W.; Schlegel, H. B.; Gill, P. M. W.; Johnson, B. G.; Robb, M. A.; Cheeseman, J. R.; Keith, T.; Petersson, G. A.; Montgomery, J. A.; Raghavachari, K.; Al-Laham, M. A.; Zakrzewski, V. G.; Ortiz, J. V.; Foresman, J. B.; Cioslowski, J.; Stefanov, B. B.; Nanayakkara, A.; Challacombe, M.; Peng, C. Y.; Ayala, P. Y.; Chen, W.; Wong, M. W.; Andres, J. L.; Replogle, E. S.; Gomperts, R.; Martin, R. L.; Fox, D. J.; Binkley, J. S.; Defrees, D. J.; Baker, J.; Stewart, J. P.; Head-Gordon, M.; Gonzalez, C.; Pople, J. A. *GAUSSIAN 94*; Gaussian, Inc.: Pittsburgh, PA, 1995.